available at www.sciencedirect.com

SCIENCE DIRECT®

journal homepage: www.elsevier.com/locate/biochempharm

Critical role of pro-apoptotic Bcl-2 family members in andrographolide-induced apoptosis in human cancer cells

Jing Zhou, Siyuan Zhang, Choon-Nam Ong, Han-Ming Shen *

Department of Community, Occupational and Family Medicine, Yong Loo Lin School of Medicine, National University of Singapore, 16 Medical Drive, Singapore 117597, Republic of Singapore

ARTICLE INFO

Article history:
Received 1 March 2006
Accepted 3 April 2006

Keywords:
Andrographolide
Bid
Bax
Bcl-2 family
Mitochondria
Apoptosis

Abbreviations:
Andro, andrographolide
CHX, cycloheximide
DAPI, 4′,6-diamidino-2-phenylindole
DMSO, dimethyl sulfoxide
PARP, poly(ADP-ribose)polymerase
PI, propidium iodide
TNFα, tumor necrosis factor α
z-DEVD-CHO, N-acetyl-Asp-Glu-Val-Asp-CHO (aldehyde)
z-IETD-FMK, benzyloxycarbonyl-Ile-Glu-Thr-Asp-(OMe) fluoromethyl ketone
z-LEHD-CHO, N-acetyl-Leu-Glu-His-Asp-CHO (aldehyde)
z-VAD-FMK, benzyloxycarbonyl-Val-Ala-Asp-(OMe) fluoromethyl ketone

ABSTRACT

Andrographolide (Andro), a diterpenoid lactone isolated from a traditional herbal medicine *Andrographis paniculata*, is known to possess potent anti-inflammatory activity. In this study, Andro induced apoptosis in human cancer cells via activation of caspase 8 in the extrinsic death receptor pathway and subsequently with the participation of mitochondria. Andro triggered a caspase 8-dependent Bid cleavage, followed by a series of sequential events including Bax conformational change and mitochondrial translocation, cytochrome c release from mitochondria, and activation of caspase 9 and 3. Inhibition of caspase 8 blocked Bid cleavage and Bax conformational change. Consistently, knockdown of Bid protein using small interfering RNA (siRNA) technique suppressed Andro-induced Bax conformational change and apoptosis. In conclusion, the pro-apoptotic Bcl-2 family members (Bid and Bax) are the key mediators in relaying the cell death signaling initiated by Andro from caspase 8 to mitochondria and then to downstream effector caspases, and eventually leading to apoptotic cell death.

* *Corresponding author*. Tel.: +65 6516 4998; fax: +65 6779 1489.
E-mail address: cofshm@nus.edu.sg (H.-M. Shen).
0006-2952/$ – see front matter
doi:10.1016/j.bcp.2006.04.019

1. Introduction

Andrographis paniculata is a traditional medicinal herb which grows widely in many Asian countries such as China, Thailand, India and Sri Lanka. For centuries, it has been widely prescribed for the treatments of various diseases, such as respiratory infection, fever, bacterial dysentery and diarrhea [1,2]. The major bioactive constituent extracted from the aerial parts of the plant is Andrographolide (Andro), a bicyclic diterpenoid lactone. As shown below, it contains an α-alkylidene γ-butyrolactone moiety and three hydroxyls at C-3, C-19 and C-14 which are responsible for the bioactivities of Andro [3]. In the last decade, various bioactivities of Andro have been described, including anti-inflammatory [4,5], anti-viral [6], and anti-hypertensive activities [7,8]. The underlying molecular mechanisms have also been investigated. For instance, nuclear transcription factor kappaB (NF-κB) is the molecular target for the anti-inflammatory activity of Andro [5,9]. Andro effectively inhibited the nuclear activation of NF-κB by covalent modification of reduced cysteine 62 of p50, to exert its potent anti-inflammatory activity [5].

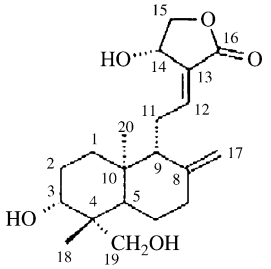

Chemical structure of Andro (C20H30O5) (3)

Andro's potent anti-inflammatory property implies the anti-cancer potential of this natural product, and such a notion is supported by a number of recent studies. For instance, Andro has been shown to inhibit cancer cell growth and its GI50 (50% growth inhibition) ranges from 10 to 28 μM, depending on the type of cancer cell tested [8]. Andro was also found to cause G0/G1 cell-cycle arrest through induction of p27 and decreased expression of cyclin-dependent kinase (CDK) 4 in some human cancer cells [10,11]. The anticancer activity of this compound is further substantiated by findings using in vivo B16F0 melanoma syngenic and HT-29 xenograft models [11]. The effect of Andro on apoptosis is controversial. Andro is capable of protecting immune cells (thymocytes) or endothelial cells against apoptosis [12,13]. On the other hand, a couple of very recent reports showed that Andro at relatively high concentrations (from 40 to 100 μM) could induce apoptosis in human prostatic adenocarcinoma PC-3 cells [14] or human leukemic HL-60 cells [15]. In both studies, Andro was shown to activate the caspase cascade; however, the detailed molecular mechanisms of Andro-induced apoptosis are still largely unknown.

Apoptosis is a cell death process that plays a critical role in development, tissue homeostasis and development of various human diseases [16]. Lack of apoptotic induction and inappropriate-controlled apoptosis process have been implicated in tumor development and progression as well as chemoresistance [17]. Two major apoptotic pathways have been identified, namely the extrinsic and the intrinsic apoptotic pathways. The extrinsic pathway is initiated *via* death receptors on cell membrane, leading to sequential activation of initiator caspases (caspase 8 or 2, 12) and effector caspases (caspase 3 and 7) [18]. In certain cell types (type I), activation of caspase 8 is sufficient for activation of caspase 3, but in great majority of cells (type II), the effector caspases activation need the amplification through mitochondria which is initiated by the cleavage of Bid by caspase 8. Among many apoptotic regulatory proteins, the Bcl-2 family, including both anti-apoptotic (Bcl-2, Bcl-X_L, Mcl-1) and pro-apoptotic members (Bid, Bax, Bad), is particularly important [19]. Moreover, it has been well established that there is a cross-talk between the death inducing signaling complex (DISC) and mitochondria via Bid, an important member of the Bcl-2 family proteins [20]. In this study, we attempted to elucidate the mechanisms involved in Andro-induced apoptosis by focusing on the functional role of the Bcl-2 family members. Results from our studies demonstrate a critical role of some pro-apoptotic Bcl-2 proteins, especially Bid and Bax in Andro-induced apoptosis. Understanding of the mechanisms of Andro-induced apoptosis could provide valuable knowledge for further investigation and development this compound into a potential anticancer agent.

2. Materials and methods

2.1. Chemicals and reagents

Andrographolide (Andro), 4′,6-diamidino-2-phenylindole (DAPI) and anti-Bax 6A7 antibodies were purchased from Sigma (St. Louis, MO, USA). Propidium iodide (PI) was purchased from Molecular Probe (Eugene, OR, USA). Anti-PARP, anti-MnSOD, anti-caspase 8, anti-caspase 3 and anti-cytochrome *c* antibodies were obtained from BD Pharmingen (San Diego, CA, USA). Anti-Bid antibody was purchased from Cell Signaling (Beverly, MA, USA) and anti-caspase 9 and anti-Bax antibodies were acquired from Chemicon (Temecula, CA, USA). Anti-tubulin antibody was obtained from Santa Cruz (Santa Cruz, CA, USA). Protease inhibitors cocktail was provided by Roche (Mannheim, Germany) and Apo-One™ Caspase 3/7 Assay Kit was from Promega (Madison, WI, USA). Bid small interfering RNA (siRNA) was purchased from QIAGEN (Valencia, CA, USA). Lipofectamine™ 2000 was obtained from Invitrogen (Carlsbad, CA, USA). pDsRed-N1 was purchased from Clontech (Palo Alto, CA, USA). The following reagents were all from BioMol (Plymouth meeting, PA, USA): pan caspase inhibitor z-VAD-FMK, caspase 3 inhibitor z-DEVD-CHO, caspase 8 inhibitor z-IETD-FMK and caspase 9 inhibitor z-LEHD-CHO.

2.2. Cell culture and treatments

Human cervical cancer cell line HeLa, human hepatoma cell line HepG2 and human breast cancer cell line MDA-MB-231 were obtained from ATCC. HeLa, HepG2 and MDA-MB-231 were maintained in DMEM medium (Sigma) with 10% FBS (Hyclone). Equal numbers of cells were seeded in DMEM medium and switched to the medium supplemented with 1% FBS for treatment. Same concentration of DMSO was always

applied to control cells. All the inhibitors were added into the wells 1 h before Andro treatment.

2.3. Detection of apoptosis

The cells undergoing apoptosis were evaluated by two methods. First, using DAPI staining to examine chromatin condensation, which are characteristics for apoptosis [21]. Briefly, after designated treatments, medium was removed and cells were fixed with 70% ethanol at room temperature for 10 min. After staining with 0.3 μg/ml DAPI (in PBS) at room temperature for 10 min, cell nuclei were visualized under an inverted fluorescence microscope and photographed (Nikon ECLIPSE TE2000-S, Nikon Instruments, Tokyo, Japan). Second, apoptotic cells were quantified using the DNA content analysis to determine the percentage of sub-G1 cells [22]. At the end of designated treatments, cells were collected and washed with PBS twice, then fixed and permeabilized in 70% ice-cold ethanol for 2 h. Fixed cells were incubated with PI staining buffer (0.1% TritonX-100, 200 μg/ml RNase A and 20 μg/ml PI in PBS) for 15 min at 37 °C followed by flow cytometry analysis.

2.4. Caspase 3/7 activity assay

Caspase 3/7 activity was examined using Apo-One™ Caspase 3/7 Assay Kit (Promega). Experiment was conducted following manufacturer's instruction. Briefly, cells were subcultured into 96-well plate in the medium containing 1% FBS for 12 h before Andro treatment. At the end of designated treatment, z-DEVD-rhodamine 110 substrate was added into the wells directly. After 4 h incubation at room temperature, the fluorescence intensity was measured by a plate reader (Tecan Spectra Flour Plus) at excitation 492 nm and emission 535 nm.

2.5. Cell subfractionation

Cell subfractionation was performed as described previously [23]. Cells were first collected and washed with cold PBS once, then resuspended in isotonic homogenization buffer (250 mM sucrose, 10 mM KCl, 1.5 mM $MgCl_2$, 1 mM Na–EDTA, 1 mM DTT, 0.1 mM PMSF, 10 mM Tris–HCl, pH 7.4) containing protease inhibitor cocktail (Roche). Cells were incubated on ice for 10 min and then passed through gauge #27 needle for 20 times to break the cell membrane. The cell homogenates were applied to a series of centrifugation at $50 \times g$ for 10 min, $500 \times g$ for 20 min and $15{,}000 \times g$ for 20 min to fractionate unbroken cells, heavy nuclear fraction and mitochondria fraction, respectively. After the final centrifugation at $100{,}000 \times g$ for 30 min, the supernatant was collected as the cytosol fraction. Equal amount of mitochondrial and cytosolic proteins were subjected to Western blot.

2.6. Immunoprecipitation and Western blot

For immunoprecipitation experiments, cells were lysed in CHAPS lysis buffer (10 mM Hepes, pH 7.4, 150 mM NaCl, 1% CHAPS) containing protease inhibitors [24]. The cell lysates were normalized for protein content and 500 μg of total protein were incubated with 2 μg of anti-Bax 6A7 monoclonal antibody (Sigma) in 500 μl of CHAPS lysis buffer overnight at 4 °C. Then, 25 μl of protein G-agarose were added into the reactions and incubated at 4 °C for an additional 3 h. After three washings in CHAPS lysis buffer, beads were boiled in loading buffer containing 5% β-mercaptoethanol and the conformational changed Bax proteins in the immunoprecipitates were subjected to Western blot analysis with anti-Bax polyclonal antibody. For Western blot, cells were first lysed in cell lysis buffer (50 mM Tris–HCl pH 8.0, 150 mM EDTA, 1% TritonX-100, 0.5% SDS and protease inhibitor cocktail) and equal amount of proteins were fractionated on SDS-PAGE gel in the Mini-PROTEAN II system (Bio-RAD) and blotted onto PVDF membrane (Millipore). After blocked with 5% nonfat milk in TBST (10 mM Tris–HCl, pH 7.5, 100 mM NaCl and 0.1% Tween-20), the membrane was probed with various antibodies and developed with enhanced chemiluminescence (Pierce) using a Kodak Image Station 440CF (Kodak). The density of the various bands in Western blot was quantified using the Kodak Image Station 440CF software (Kodak).

2.7. Transient transfection and small interfering RNA-mediated protein knockdown

HeLa cells were seeded in 12-well plate overnight before the transfection. Cells were co-transfected with pcDNA3.1 control vector, Bcl-2 expression vector or CrmA expression vector (a kind gift from Dr. Z.G. Liu, NCI, USA) together with the pDsRed-N1 vector (Clontech) using Lipofectamine™ 2000 (Invitrogen) according to manufacture's recommendations. For siRNA experiments, negative control siRNA, and validated siRNA duplex targeting human Bid and Lamin A/C were purchased from QIAGEN. The cellular delivery of siRNA was carried out by using Lipofectamine™ 2000 and optimized with various doses and post-transfection time and evaluated by Western blot. HeLa cells were first seeded in DMEM medium without antibiotics in a 24-well plate overnight before transfection. Ready-to-use siRNA was mixed with 50 μl medium containing appropriate amount of Lipofectamine™ 2000 (1 μl/well) to achieve a final concentration of siRNA at 10 nM. The mixture was incubated at room temperature for 20 min to allow the formation of transfection complexes. The formed mixture was then added into the well and incubated for 4 h before it was replaced by fresh DMEM medium. The transfected cells were treated with Andro 72 h after transfection, and apoptotic cell death was evaluated by DAPI staining.

2.8. Immunofluorescence and confocal microscopy

HepG2 cells were seeded in eight-well chamber slides 24 h before treatment. At the end of treatments, cells were washed with PBS and fixed in 3% paraformaldehyde for 1 h. After permeablized for 2 min with 0.2% CHAPS in PBS, cells were blocked in 2% BSA with 0.2% Tween-20 for 30 min and further incubated with anti-Bax 6A7 antibody overnight at 4 °C. After washed with PBS (+0.2% Tween-20), cells were incubated with anti-mouse Alexa 633 secondary antibody for another 1 h. Cover slips were mounted onto slides using ProLong anti-fade mounting reagent (Molecular Probes). Cells were visualized under Olympus FLOVIEW V500 confocal microscope. The intensity of Bax 6A7 staining was measured in 10 randomly

selected fields with Image-Pro-Plus (Media Cybernetics) and the relative fluorescence intensities (arbitrary unit) were presented as means ± S.D.

2.9. Statistical analysis

All numerical data were presented as means ± S.D. from at least three independent experiments. Student's *t*-test was used to analyze statistical difference. *p*-Values less than 0.05 were considered significant.

3. Results

3.1. Andrographolide induces apoptosis in human cancer cells

To explore anti-cancer potential of Andro, three types of human cancer cell lines (human hepatoma cancer cell HepG2, human cervical cancer cell HeLa and human breast cancer cell MDA-MB-231) were treated with different concentrations of Andro. After 24 h treatment, the apoptotic cell death induced by Andro was identified by typical nuclear condensation visualized with DAPI staining. Fig. 1A demonstrated a dose-dependent pattern of Andro-induced apoptotic cell death in three cancer cell lines. Andro-induced apoptosis was further examined using DNA content analysis. As shown in Fig. 1B, in HepG2 cells the dose-dependent increase of sub-G1 cells was basically consistent with the results in Fig. 1A. Furthermore, a typical 87 kDa PARP cleavage product, a hallmark of apoptosis [25], was observed in HepG2 cells upon Andro treatment in a time- and dose-dependent manner (Fig. 1C). Similar results were also found in HeLa cells (data not shown).

3.2. A caspase cascade in Andro-induced apoptosis

To determine the involvement of caspase cascade in Andro-induced apoptosis, we first examined the caspase activation by performing Apo-One™ Caspase 3/7 assay. As shown in Fig. 2A, around eight-fold increases of caspase 3/7 activity were observed after treatment with Andro for 12 h. Cells treated with TNFα were used as a positive control. Consistent with this observation, the cleavage of caspase 3 from proform into its active form (p17) was detected by Western blot after Andro treatments (Fig. 2B). In order to determine the involvement of the initiator caspases upstream of caspase 3, we measured the activation of the two initiator caspases: caspase 8 in the death receptor pathway and caspase 9 in the mitochondrial pathway. A dose-dependent cleavage of caspase 8 and decrease of proform of caspase 9 were detected (Fig. 2B). The involvement of the caspase cascade in Andro-induced apoptosis was further studied by applying different caspase inhibitors in Andro-treated cells. Both pan-caspase inhibitor z-VAD-FMK and the specific inhibitors for caspases 8, 9 and 3 could effectively block the PARP cleavage (Fig. 2C) as well as Andro-induced apoptotic cell death as detected by DAPI staining (Fig. 2D). All these findings demonstrated that Andro-induced apoptosis involves key caspases in both the extrinsic death receptor pathway and the mitochondria-dependent pathway.

3.3. Andro induces Bid cleavage following caspase 8 activation

It has been well established that Bcl-2 family proteins play pivotal roles in regulation of apoptotic pathways [26]. Among these proteins, Bid, a pro-apoptotic Bcl-2 family member, provides a critical step cross-linking the extrinsic cell death receptor signaling pathway to mitochondria upon caspase 8-mediated cleavage [20]. In this study, activation of the two initiator caspase 8 and 9 prompted us to examine the involvement of Bid and other Bcl-2 family members in Andro-induced apoptosis. After the treatment with Andro, we first observed a dose- and time-dependent decrease of full length Bid protein (Fig. 3A). More importantly, as shown in Fig. 3B, when cells were pretreated with pan-caspase inhibitor (z-VAD-FMK) or caspase 8 inhibitor (z-IETD-FMK), the decrease of full length of Bid caused by Andro was prevented, suggesting that Bid cleavage is mediated by caspase 8 activation.

3.4. Andro induces Bax conformational change

It has been reported that pro-apoptotic Bax is closely related with Bid and undergoes a conformational change and consequent mitochondrial translocation during apoptosis [27]. In this study, we examined the Bax changes induced by Andro treatment. By using the Bax (6A7) monoclonal antibody, which specifically recognizes the Bax protein with conformational change but not the native form [28], there was a time-dependent increase of Bax staining in Andro-treated cells, suggesting the conformational change of Bax (Fig. 4A). Being consistent with this observation, we also detected the increase of Bax protein with conformational changes using immunoprecipitation with the Bax (6A7) antibody (Fig. 4B). Furthermore, as shown in Fig. 4C, Bax conformational changes were proven to be caspase 8-dependent, as pretreatment with caspase 8 inhibitor (z-IETD-FMK) almost completely abolished the Andro-induced conformational changes of Bax.

3.5. Andro induces Bax translocation and cytochrome c release

To further examine the effect of Andro on mitochondria, we studied the mitochondrial translocation of Bax (Fig. 5A) and the release of cytochrome *c* from the mitochondria (Fig. 5B). Starting from 4 h, there was a time-dependent progressive increase of Bax in the mitochondrial fraction and the concurrent increase of cytochrome *c* release from mitochondria to the cytosol in the Andro-treated cells. Such a finding is consistent with the previous reports that the integration of Bax in the outer membrane followed by cytochrome *c* release is a possible prerequisite for mitochondrial apoptotic pathway [29].

3.6. Knockdown of Bid expression protects cell from Andro-induced cell death

In order to confirm the critical role of Bid in Andro-induced apoptotic cell death, we manipulated Bid protein level by using siRNA technology. Transient transfection of siRNA duplex

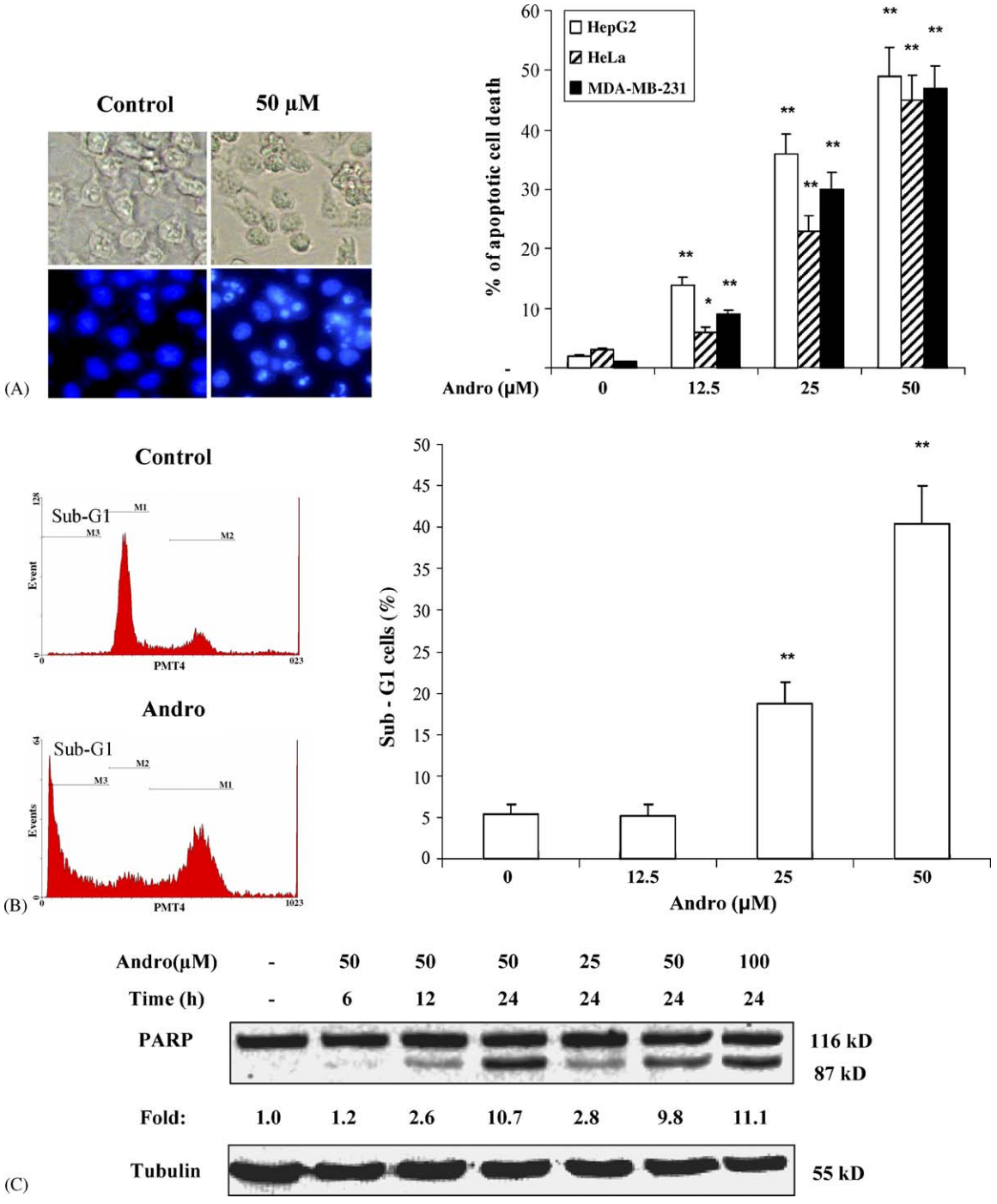

Fig. 1 – Andro induces apoptosis in human cancer cell lines. (A) Nuclear condensation in apoptotic cells detected by DAPI staining. HepG2, HeLa and MDA-MB-231 cells were treated with various concentrations of Andro for 24 h. The result was presented as the percentage of cells with evident nuclear condensation in 200 randomly selected cells. Inserted are representative images of HeLa cells photographed under a normal light microscope (upper panel) or cells with DAPI staining visualized under an inverted fluorescence microscope (lower panel). (B) Flow cytometry analysis shows the percentage of sub-G1 in HepG2 cells treated with Andro for 24 h. Inserted are typical histograms showing the sub-G1 peak in Andro-treated cells. (C) Dose-dependent and time-dependent cleavage of PARP was induced by Andro. HepG2 cells were treated with designated concentrations of Andro for 6, 12 or 24 h, and the PARP cleavage was detected by Western blot. The 87 kDa band was quantified and the fold of increase was presented. In both (A and B), data were presented as mean ± S.D. from three independent experiments and analyzed by using Student's *t*-test ($^{**}p < 0.01$ when compared to the control group).

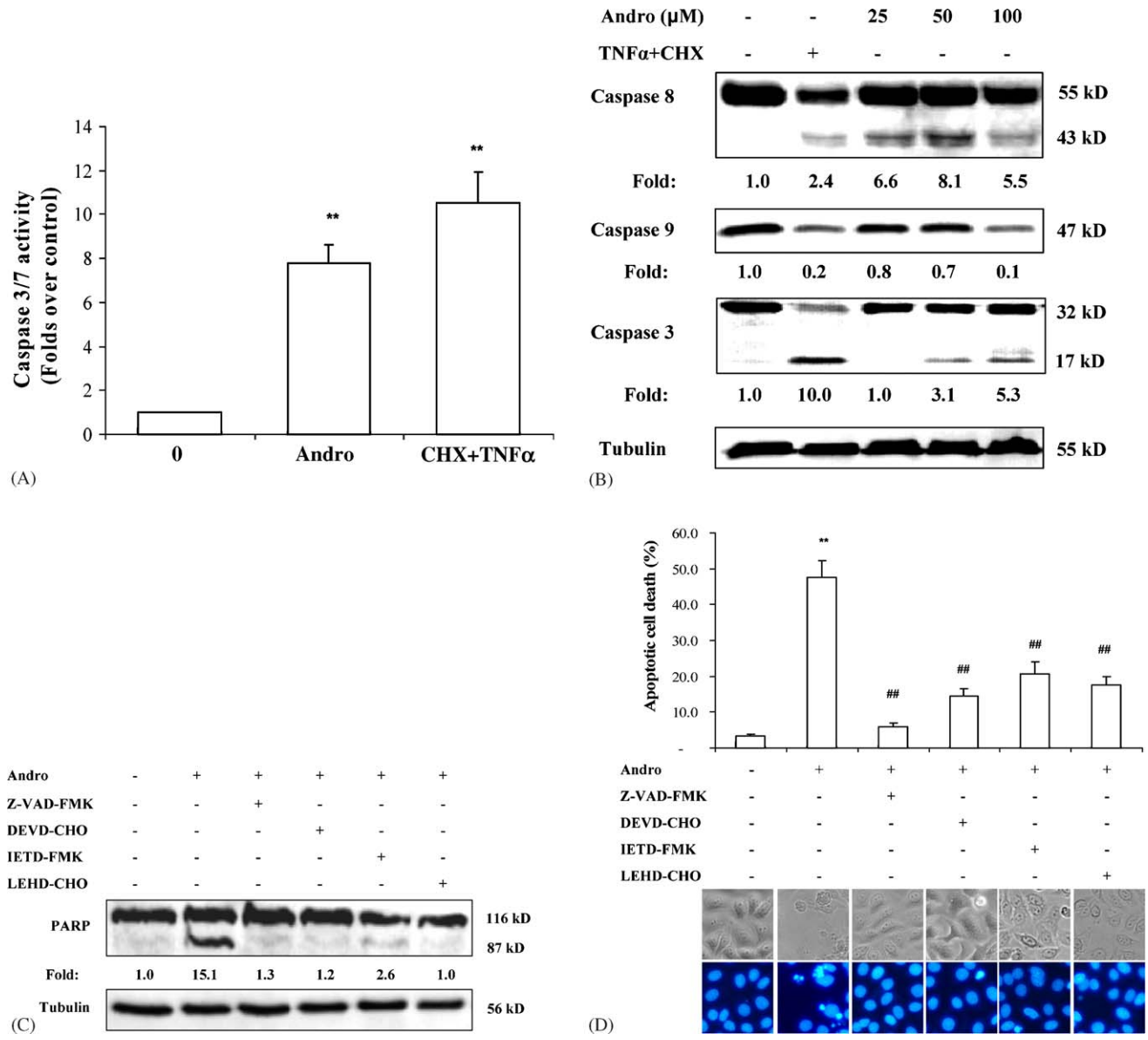

Fig. 2 – Involvement of caspase cascade in Andro-induced apoptosis in HepG2 cells. (A) Caspase 3/7 like activity was measured by Apo-One™ Caspase 3/7 Assay Kit. HepG2 cells were cultured in the 96-well plate and treated with Andro (50 μM) for 6 h. TNFα (20 ng/ml + CHX 25 ng/ml) for 6 h was used as a positive control. (B) Andro-induced caspase 8, 9 and 3 cleavages were detected by Western blot. HepG2 cells were treated with Andro at indicated concentrations for 24 h. Treatment with CHX + TNFα for 6 h was used as a positive control. (C) Inhibition of Andro-induced PARP cleavage by caspase inhibitors. HepG2 cells were pretreated with z-VAD-FMK (25 μM), z-DEVD-CHO (50 μM), z-LETD-FMK (50 μM) or z-LEHD-CHO (50 μM), respectively, for 1 h followed with Andro (50 μM) treatment for 24 h. PARP cleavage was detected by Western blot. (D) Suppression of Andro-induced apoptosis by caspase inhibitors. Apoptotic cell death was evaluated by DAPI staining as described in Fig. 1. The numeric data were presented as mean ± S.D. from at least three independent experiments ($^{**}p < 0.01$ when compared to control group; $^{\#\#}p < 0.01$ when compared to the Andro-treated only group). In (B and C), the densities of the respective cleaved band of caspase 8, 3 and PARP and the proform of capsase 9 were quantified and the folds of increase were presented accordingly. Tubulin was blotted as a loading control.

specifically targeting human Bid gene resulted in a significant reduction of Bid protein level comparing to the negative control siRNA transfection (Fig. 6A). As a result, there was no pronounced Bax staining (by Bax 6A7 antibody) in Bid siRNA transfected cells (Fig. 6B) different from the observation on the negative control siRNA transfected cells, suggesting that the Bax conformational changes were triggered by Bid cleavage following Andro treatment. Moreover, knockdown of Bid protein level also offered significant resistance to Andro-induced apoptosis (Fig. 6C), which supports the notion that Bid–Bax signaling plays a critical role in Andro-induced apoptosis.

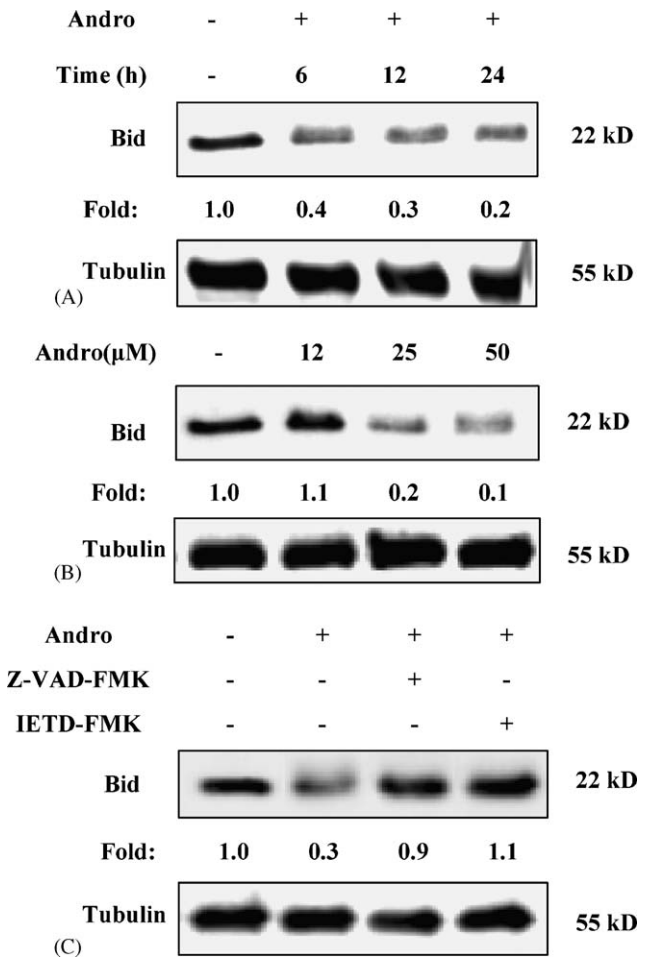

Fig. 3 – Andro-induced Bid cleavage following caspase 8 activation in HepG2 cells. (A) Andro-induced Bid cleavage detected by Western blot. HepG2 cells were treated with Andro (50 μM) for indicated times (upper panel). In the lower panel, HepG2 cells were treated with Andro in designated concentrations for 6 h. (B) Andro-induced Bid cleavage was blocked by caspase inhibitors. HepG2 cells were pretreated with caspase 8 inhibitor (z-IETD-FMK) or pan-caspase inhibitor (z-VAD-FMK) for 1 h, followed by Andro (50 μM) treatment for another 6 h. The density of the Bid band was quantified and the fold of increase was presented. Tubulin was blotted as a loading control.

3.7. *Bcl-2 and CrmA over-expression block Andro-induced apoptosis*

In addition to pro-apoptotic Bcl-2 family proteins, we further examined the involvement of the anti-apoptotic Bcl-2 protein. It is known that Bcl-2 is a mitochondrial protein that inhibits apoptotic process and promotes cell survival by heterodimerization with pro-apoptotic Bcl-2 family members such as Bax [30,31]. As shown in Fig. 7, over-expression of Bcl-2 effectively inhibited the Andro-induced apoptotic death. This observation strongly supports the notion that Bcl-2 family members including both the anti-apoptotic and pro-apoptotic proteins are critical regulators in Andro-induced apoptosis. Finally, in order to confirm the initiating function of caspase 8 activation in the mitochondrial apoptotic pathway induced by Andro, we overexpressed a specific caspase 8 inhibitor protein (CrmA) in HeLa cells. In Fig. 7A, those successfully transfected cells were marked in red and the living cells maintained the normal morphology while the dead cells appeared rounded and shrinked. It is evident that over-expression of CrmA protein remarkably protected the cell from apoptotic death caused by Andro. The above data were quantified by counting the percentage of dead cells among the transfected cells (Fig. 7B). Data from this part of the experiment further demonstrate that Andro is capable of utilizing the death receptor pathway in the induction of apoptotic cell death in human cancer cells.

4. Discussion

Although the medicinal herb *Andrographis paniculata* has been used for centuries as an anti-inflammatory medicine, its anti-cancer property has not been well studied. Recently, Andro, the main active component of this herbal medicine, has been found to be able to inhibit cancer cell proliferation [10], induce cell-cycle arrest [10,11] and promote apoptosis [14,15] in human cancer cells. For example, Andro caused apoptotic morphological change and caspase 3, 8 activations in PC-3 cells [14]. In HL-60 cells, Andro treatment induced mitochondrial cytochrome *c* release, accompanied by increased expression level of Bax and decreased expression level of Bcl-2 protein [15]. However, there are a number of important issues regarding the effect of Andro on apoptosis remaining to be further elucidated. First, Andro may inhibit or promote apoptosis depending on various factors such as the cell type and the nature of the apoptotic stimuli. For instance, Andro is capable of protecting endothelial cells against apoptosis induced by growth factor deprivation via activation of the PI3K-AKT pathway [12]. Second, the molecular mechanism underlying Andro-induced apoptosis in cancer cells has not been fully investigated. In this study, we examined the mechanisms of Andro-induced apoptosis by focusing on the caspase cascade and the regulatory role of the Bcl-2 family members. The results from this study suggest that Andro-induced apoptotic cell death by the receptor apoptotic pathway leads to the apoptotic activation of mitochondria which facilitates the release of apoptotic factors and thus amplifies the caspase cascade. More importantly, Bid and Bax, two pro-apoptotic Bcl-2 family members are critical mediators relaying the death signal from the initiator caspase 8 to caspase 9 and eventually the effector caspase 3 and apoptotic cell death in cancer cells.

One intriguing finding from this study is that the apoptotic cell death induced by Andro was initiated by the extrinsic death receptor pathway, based on the observations that Andro activated caspase 8 and both synthetic caspase 8 inhibitor (z-IETD-fmk) (Fig. 2) and CrmA, a viral caspase 8 inhibitory protein [32], were able to prevent Andro-induced apoptosis (Fig. 7). Such a mechanism of action by Andro is indeed similar to a number of other natural products that have been shown to induce apoptotic *via* the death receptor apoptotic pathway. For instance, ajoene, an extract from garlic, kills HL-60 cells via activation of the initiator caspase 8 [33]. Prodelphinidin B-2,3,3′-di-O-gallate from *Myrica rubra* induces the apoptosis in

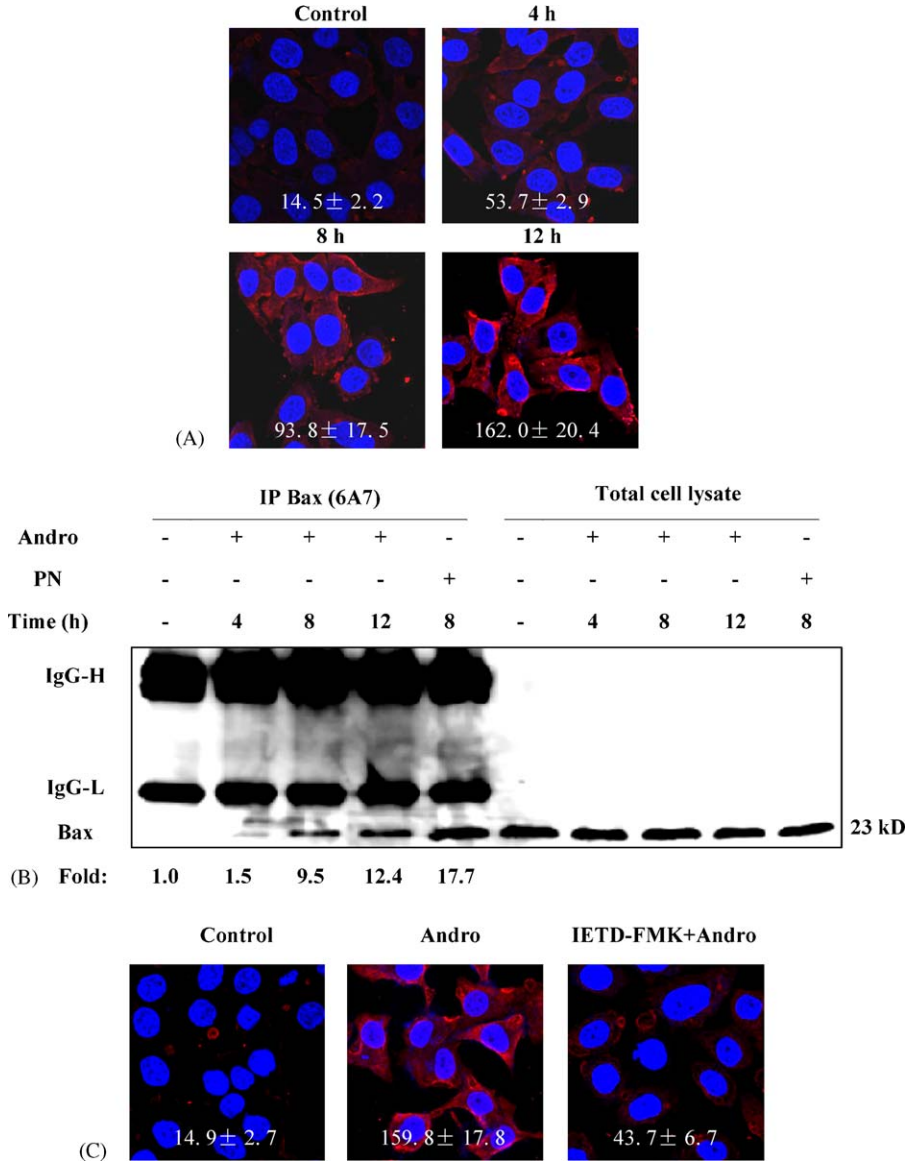

Fig. 4 – Bax conformational change following caspase 8 activation in HepG2 cells. (A) Conformational changes of Bax detected by immunofluorescence staining. Following treatment with Andro (50 μM) for indicated time, Bax conformational changes were determined by immunofluorescence staining using a mouse anti-Bax 6A7 antibody. HepG2 cells were counterstained with DAPI to visualize nuclei. Images are representatives of three individual experiments. (B) Conformational changes of Bax detected by immunoprecipitation and Western blot. HepG2 cells were treated as panel A and subjected to immunoprecipitation with anti-Bax 6A7 monoclonal antibody followed by Western blot analysis with anti-Bax polyclonal antibody. Treatment with parthenolide (25 μM) for 8 h was used as positive control [23]. The density of the Bax band was quantified and the fold of increase was presented. In addition, the total lysates (40 μg of protein per lane) were blotted directly. (C) Bax conformational changes blocked by a caspase 8 inhibitor. HepG2 cells were treated with Andro (50 μM) in the presence (+) or absence (−) of caspase 8 inhibitor (z-IETD-FMK), following the same protocol as in panel A for Bax staining. In (A and C), the intensity of Bax 6A7 staining was measured in 10 randomly selected fields and the relative fluorescence intensities (arbitrary unit) were presented as mean ± S.D.

MCF-7 cells through the Fas/FasL system [34]. Similarly, the apoptosis triggered by the water extract of *Phyllanthus urinaria* is also mediated through Fas ligand/receptor [35]. The exact mechanisms by which the extrinsic apoptosis pathway is activated by those natural products are mostly elusive. One possibility involves the enhanced expression of both the death receptor and the ligand [35]. In this study, Andro did not alter the expression of death receptor DR4 and DR5 in both HepG2 and HeLa cells (data not shown), thus it remains to be further determined how Andro acts on the death receptor and the ligand. Another possibility is that Andro may augment caspase 8 activation via its inhibitory effect on NF-κB activation, based on an earlier observation that Andro is able to inhibit NF-κB by covalent modification of reduced cysteine 62 of p50 in immuno

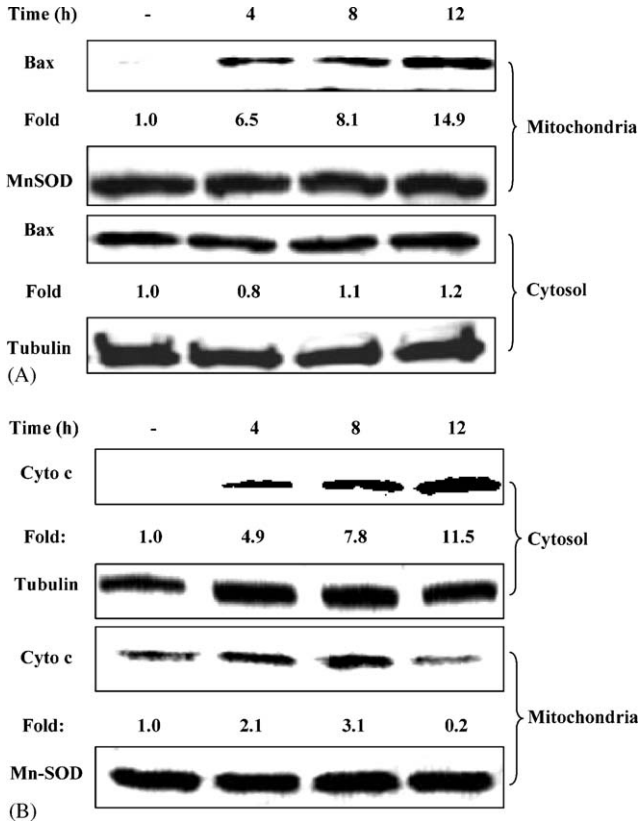

Fig. 5 – Andro induces Bax mitochondrial translocation and cytochrome *c* release in HepG2 cells. (A) Mitochondrial translocation of Bax. HepG2 cells were exposed to Andro (50 μM) for 0, 4, 8 or 12 h and subjected to subcellular fractionation for mitochondria-rich fraction and cytosol. (B) Cytochrome *c* release upon Andro treatments. HepG2 cells were treated with Andro (50 μM) for 4, 8 or 12 h, respectively and cytosolic fraction was subject to Western blot for detection of cytochrome *c* release. MnSOD and tubulin were used as loading controls for the mitochondrial and cytosolic fractions, respectively.

cells [5]. It has been well established that NF-κB is generally acting as a powerful anti-apoptotic factor via up-regulation of an array of anti-apoptotic genes [36]. One of such target genes is cellular FLICE-inhibitory protein (c-FLIP) which is capable of directly inhibiting caspase 8 activation [37]. Therefore, suppression of NF-κB signaling pathway will lead to down-regulation of c-FLIP and increased activation of caspase 8 [38]. In this study, Andro did not affect the basal level of NF-κB activation in the cancer cells tested (data not shown). Nevertheless, it remains to be further investigated whether the inhibitory effect of Andro on NF-κB is involved in apoptosis in cells with stimulated NF-κB pathway.

An earlier study by Kim and Milner on Andro provided some preliminary evidence showing the activation of caspase 8 and caspase 3, without examining the detailed mechanism contributing to Andro-induced apoptosis [14]. In this study, we further examined the apoptotic cell death process following the activation of the initiator caspase 8. It was found that the protein level of full length Bid was significantly decreased upon Andro treatment (Fig. 3A). As expected, such a change was prevented by the pretreatment of the caspase 8 inhibitor z-IETD-FMK and the pan-caspase inhibitor z-VAD-FMK (Fig. 3B), suggesting that caspase 8 was responsible for Bid cleavage in Andro-treated cells. It has been well established that caspase 8-mediated Bid cleavage and subsequent Bid mitochondrial translocation mediate mitochondria alteration in response to activation of cell surface death receptor [39,40]. One of the key molecules in response to Bid cleavage and mitochondrial translocation is Bax: Bax undergoes transformation and oligomerization to form pores in the outer mitochondrial membrane, leading to the release of pro-apoptotic proteins from mitochondria, such as cytochrome *c* [19,27]. Therefore, we next focused on the involvement of Bax in Andro-induced apoptosis, with the following observations: first, there was a striking conformational change of Bax detected in Andro-treated cells with the conformation-specific antibody 6A7 in both immunohistochemistry staining (Fig. 4A) and immunoprecipitation assay (Fig. 4B). Second, in the cell fractionation experiments, significant amount of Bax accumulated in mitochondria following Andro treatment (Fig. 5A). Different from an earlier observation in which Andro enhanced Bax protein expression [15], no change of the total Bax protein level was found in our study (data not shown) suggesting that Andro-induced apoptosis is mainly regulated via Bid cleavage-associated Bax transformational alteration, but not via up-regulation of Bax. At present the mechanisms underlying such discrepancy are not known. It is possible that Andro is capable of enhancing the pro-apoptotic function of Bax via multiple mechanisms.

As mentioned above, Bax has been considered as one of the most important pro-apoptotic Bcl-2 members promoting mitochondrial apoptotic pathway [27]. One important underlying mechanism of the pro-apoptotic function of Bax is to promote the release of pro-apoptotic factors such as cytochrome *c* from mitochondria [29,41]. It has been proposed that Bax may stimulate the opening of the permeability transition pore (PTP) through interaction with the adenine nucleotide translocator. As a result of PTP opening, mitochondria would swell, leading to rupture of the outer mitochondrial membrane and release of cytochrome *c* [29]. In this study, Bax mitochondrial translocation was accompanied by the concurrent release of cytochrome *c* in Andro-treated cells (Fig. 5B). Furthermore, it is known that Bax's proapoptotic activity is subject to the regulation by other Bcl-2 family members. For instance, the anti-apoptotic Bcl-2 protein is able to block apoptosis by binding to Bax to form Bcl-2–Bax heterodimers [31]. In our study, overexpression of Bcl-2 protein offered significant protection against Andro-induced apoptosis (Fig. 7). Andro has been shown to down-regulate the expression of Bcl-2 protein [15]. It is thus believed that in Andro-treated cells, the pro-apoptotic function of Bid and Bax overruns the anti-apoptotic function of Bcl-2, leading to apoptosis.

In order to further elucidate the role of Bid–Bax in Andro-induced apoptosis, we manipulated the Bid protein level by using the siRNA technology. It is clear that the knockdown of Bid protein level gave rise to two important consequences:

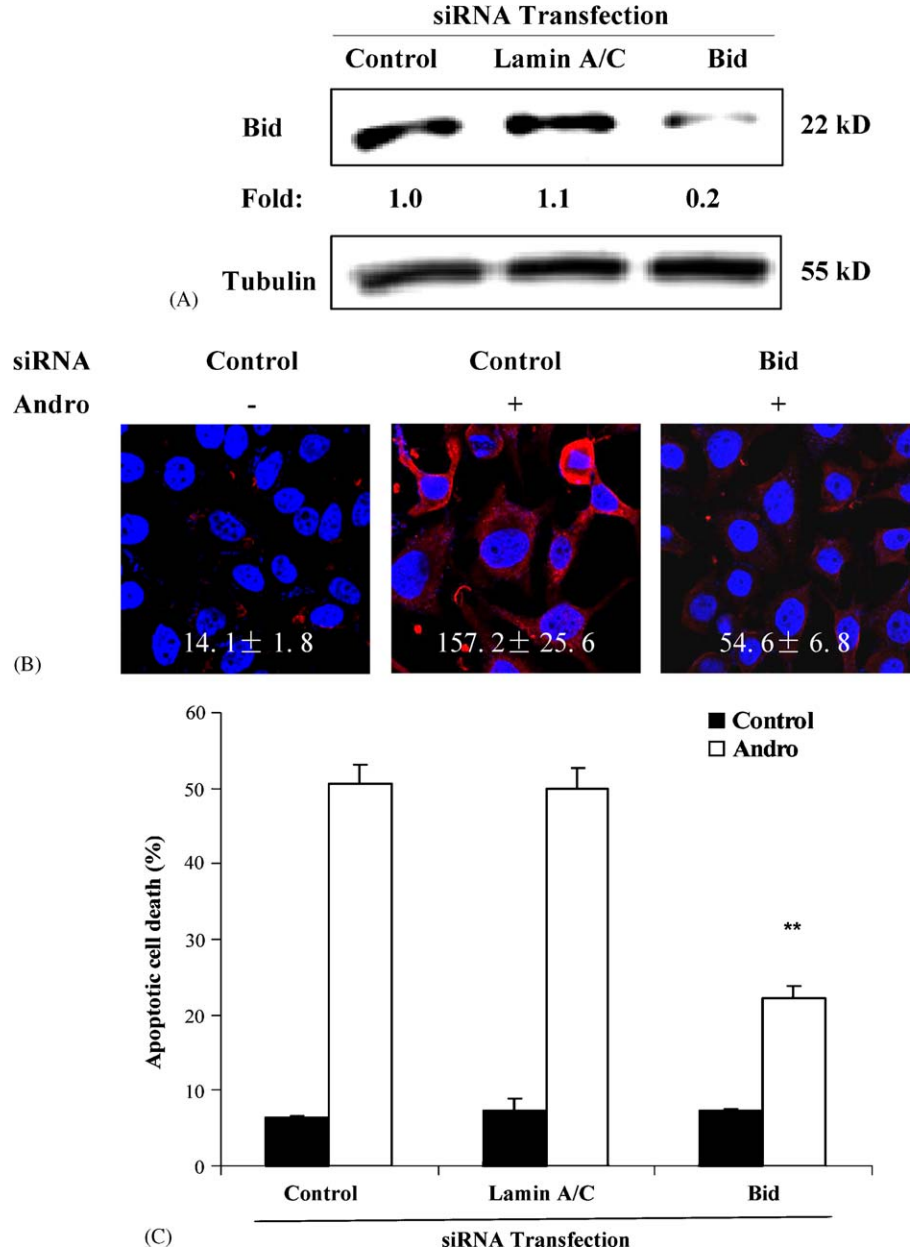

Fig. 6 – Knockdown of Bid expression protects cell from Andro-induced cell death in HeLa cells. (A) Reduction of Bid protein level by siRNA. HeLa cells were transfected with various siRNA duplexes for 72 h and Bid protein level were evaluated by Western blot. (B) Down-regulation of Bid inhibited the Bax conformational changes. HeLa cells were first transfected with various siRNA duplexes as described above, followed by Andro (50 μM) treatment for 12 h. The conformational changes of Bax were visualized by immunofluorescence as mentioned in Fig. 4. (C) Inhibition of Andro-induced apoptosis by down-regulation of Bid. HeLa cells were transfected with different siRNA duplexes as described above, and then subjected to Andro (50 μM) treatment for 24 h. Cells under apoptotic cell death were counted under an inverted fluorescence microscope after DAPI staining (mean ± S.D. from at least three independent experiments, $^{**}p < 0.01$ when compared to the control group).

reduction of Bax transformation (Fig. 6B) and protection from apoptotic cell death (Fig. 6C). These results thus strengthen our argument that Bid and Bax play key role in the apoptotic signaling initiated by Andro. Although our data clearly suggest that Bid is a critical upstream regulator of the pro-apoptosis function of Bax, Bax activation and translocation also can be initiated by other mechanisms: (i) direct activation of Bax by Bim [27]; (ii) enhanced Bax expression induced by tumor suppressor p53 [42,43]. Further studies are required to elucidate the role of other Bcl-2 family members in Andro-induced apoptosis.

Taking together, data from this study provide convincing evidence that the pro-apoptotic Bcl-2 family members (Bid and Bax) are the key mediators in relaying the cell death signaling

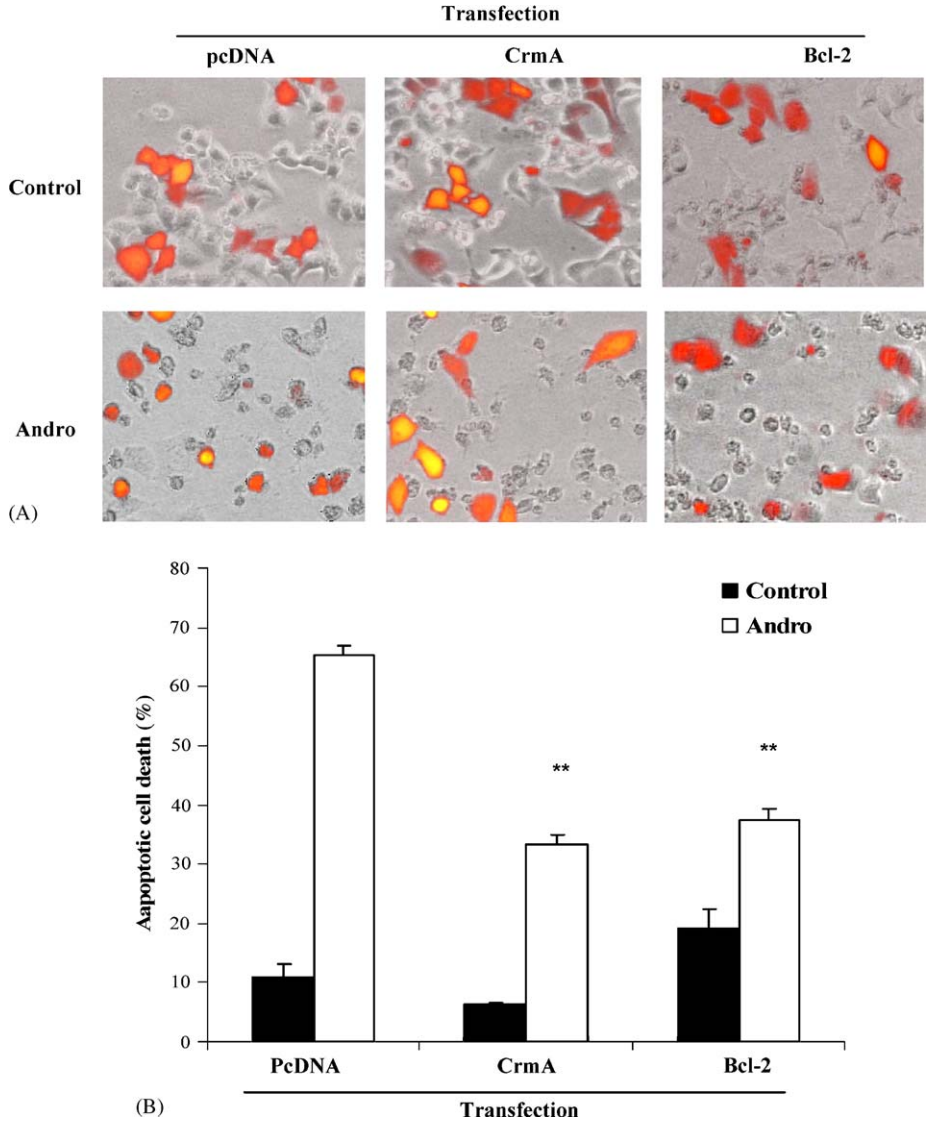

Fig. 7 – Ectopic expression of Bcl-2 and CrmA blocks Andro-induced apoptosis in HeLa cells. (A) HeLa cells were transiently transfected with pcDNA, CrmA or Bcl-2, together with pDsRed as a transfection marker. 48 h after transfection, cells were treated with Andro (50 μM) for another 24 h. Cell death was then evaluated by morphological changes under a fluorescent microscope and those successfully transfected cells were in bright red. (B) Quantification of cell death by counting the percentage of dead cells in total of randomly selected 200 transfected cells. Data are presented as mean ± S.D. from three independent transfection experiments ($^{**}p < 0.01$ when compared to control group). "For interpretation of the references to color in this figure legend, the reader is referred to the web version of the article".

initiated by Andro from caspase 8 to mitochondria and then to downstream effector caspase, and eventually leading to apoptotic cell death. Understanding the molecular mechanisms underlying Andro-induced apoptosis in cancer cells may provide new insights for further investigation and development of Andro into a potential anticancer agent.

Acknowledgement

This work was supported in part by research grants from the Academic Research Fund, National University of Singapore (NUS). J. Zhou was supported by a research scholarship from NUS and S. Zhang was supported by the Provost Fund from NUS. The authors thank Mr. Y.B. Ong and Ms. M. Zhao for their technical assistance.

REFERENCES

[1] Poolsup N, Suthisisang C, Prathanturarug S, Asawamekin A, Chanchareon U. Andrographis paniculata in the symptomatic treatment of uncomplicated upper respiratory tract infection: systematic review of randomized controlled trials. J Clin Pharm Ther 2004;29: 37–45.

[2] Iruretagoyena MI, Tobar JA, Gonzalez PA, Sepulveda SE, Figueroa CA, Burgos RA, et al. Andrographolide interferes with T cell activation and reduces experimental autoimmune encephalomyelitis in the mouse. J Pharmacol Exp Ther 2005;312:366–72.
[3] Nanduri S, Nyavanandi VK, Thunuguntla SS, Kasu S, Pallerla MK, Ram PS, et al. Synthesis and structure–activity relationships of andrographolide analogues as novel cytotoxic agents. Bioorg Med Chem Lett 2004;14: 4711–7.
[4] Panossian A, Davtyan T, Gukassyan N, Gukasova G, Mamikonyan G, Gabrielian E, et al. Effect of andrographolide and Kan Jang-fixed combination of extract SHA-10 and extract SHE-3 on proliferation of human lymphocytes, production of cytokines and immune activation markers in the whole blood cells culture. Phytomedicine 2002;9:598–605.
[5] Xia YF, Ye BQ, Li YD, Wang JG, He XJ, Lin X, et al. Andrographolide attenuates inflammation by inhibition of NF-kappa B activation through covalent modification of reduced cysteine 62 of p50. J Immunol 2004;173:4207–17.
[6] Reddy MK, Reddy MV, Gunasekar D, Murthy MM, Caux C, Bodo B. A flavone and an unusual 23-carbon terpenoid from *Andrographis paniculata*. Phytochemistry 2003;62:1271–5.
[7] Jain DC, Gupta MM, Saxena S, Kumar S. LC analysis of hepatoprotective diterpenoids from *Andrographis paniculata*. J Pharm Biomed Anal 2000;22:705–9.
[8] Kumar RA, Sridevi K, Kumar NV, Nanduri S, Rajagopal S. Anticancer and immunostimulatory compounds from *Andrographis paniculata*. J Ethnopharmacol 2004;92:291–5.
[9] Hidalgo MA, Romero A, Figueroa J, Cortes P, Concha II, Hancke JL, et al. Andrographolide interferes with binding of nuclear factor-kappaB to DNA in HL-60-derived neutrophilic cells. Br J Pharmacol 2005;144:680–6.
[10] Satyanarayana C, Deevi DS, Rajagopalan R, Srinivas N, Rajagopal S. DRF 3188 a novel semi-synthetic analog of andrographolide: cellular response to MCF 7 breast cancer cells. BMC Cancer 2004;4:26.
[11] Rajagopal S, Kumar RA, Deevi DS, Satyanarayana C, Rajagopalan R. Andrographolide, A potential cancer therapeutic agent isolated from *Andrographis paniculata*. J Exp Ther Oncol 2003;3:147–58.
[12] Chen JH, Hsiao G, Lee AR, Wu CC, Yen MH. Andrographolide suppresses endothelial cell apoptosis via activation of phosphatidyl inositol-3-kinase/Akt pathway. Biochem Pharmacol 2004;67:1337–45.
[13] Burgos RA, Seguel K, Perez M, Meneses A, Ortega M, Guarda MI, et al. Andrographolide inhibits IFN-gamma and IL-2 cytokine production and protects against cell apoptosis. Planta Med 2005;71:429–34.
[14] Kim YS, Milner JA. Targets for indole-3-carbinol in cancer prevention. J Nutr Biochem 2005;16:65–73.
[15] Cheung HY, Cheung SH, Li J, Cheung CS, Lai WP, Fong WF, et al. Andrographolide isolated from *Andrographis paniculata* induces cell cycle arrest and mitochondrial-mediated apoptosis in human leukemic HL-60 cells. Planta Med 2005;71:1106–11.
[16] Fadeel B, Orrenius S. Apoptosis: a basic biological phenomenon with wide-ranging implications in human disease. J Int Med 2005;258:479–517.
[17] Gatti L, Zunino F. Overview of tumor cell chemoresistance mechanisms. Methods Mol Med 2005;111:127–48.
[18] Natoni F, Diolordi L, Santoni C, Gilardini Montani MS. Sodium butyrate sensitises human pancreatic cancer cells to both the intrinsic and the extrinsic apoptotic pathways. Biochim Biophys Acta 2005;1745:318–29.
[19] Cory S, Adams JM. The Bcl2 family: regulators of the cellular life-or-death switch. Nat Rev Cancer 2002;2:647–56.
[20] Danial NN, Korsmeyer SJ. Cell death: critical control points. Cell 2004;116:205–19.
[21] Hunter AL, Choy JC, Granville DJ. Detection of apoptosis in cardiovascular diseases. Methods Mol Med 2005;112:277–89.
[22] Darzynkiewicz Z, Bruno S, Del Bino G, Gorczyca W, Hotz MA, Lassota P, et al. Features of apoptotic cells measured by flow cytometry. Cytometry 1992;13:795–808.
[23] Zhang S, Ong CN, Shen HM. Involvement of proapoptotic Bcl-2 family members in parthenolide-induced mitochondrial dysfunction and apoptosis. Cancer Lett 2004;211:175–88.
[24] Yamaguchi H, Paranawithana SR, Lee MW, Huang Z, Bhalla KN, Wang HG, et al. B analogue (BMS-247550)-mediated cytotoxicity through induction of Bax conformational change in human breast cancer cells. Cancer Res 2002;62:466–71.
[25] D'Amours D, Desnoyers S, D'Silva I, Poirier GG. Poly (ADP-ribosyl)ation reactions in the regulation of nuclear functions. Biochem J 1999;342(Pt 2):249–68.
[26] Rupniewska Z, Bojarska-Junak A. Apoptosis: mitochondrial membrane permeabilization and the role played by Bcl-2 family proteins. Postepy Hig Med Dosw (Online) 2004;58:538–47.
[27] Kuwana T, Bouchier-Hayes L, Chipuk JE, Bonzon C, Sullivan BA, Green DR, et al. BH3 domains of BH3-only proteins differentially regulate Bax-mediated mitochondrial membrane permeabilization both directly and indirectly. Mol Cell 2005;17:525–35.
[28] Hsu YT, Youle RJ. Nonionic detergents induce dimerization among members of the Bcl-2 family. J Biol Chem 1997;272:13829–34.
[29] Eskes R, Desagher S, Antonsson B, Martinou JC. Bid induces the oligomerization and insertion of Bax into the outer mitochondrial membrane. Mol Cell Biol 2000;20:929–35.
[30] Hengartner MO. The biochemistry of apoptosis. Nature 2000;407:770–6.
[31] Yi X, Yin XM, Dong Z. Inhibition of Bid-induced apoptosis by Bcl-2. tBid insertion, Bax translocation, and Bax/Bak oligomerization suppressed. J Biol Chem 2003;278:16992–9.
[32] Muzio M, Salvesen GS, Dixit VM. FLICE induced apoptosis in a cell-free system: cleavage of caspase zymogens. J Biol Chem 1997;272:2952–6.
[33] Dirsch VM, Antlsperger DS, Hentze H, Vollmar AM. Ajoene an experimental anti-leukemic drug: mechanism of cell death. Leukemia 2002;16:74–83.
[34] Kuo PL, Hsu YL, Lin TC, Lin LT, Lin CC. Induction of apoptosis in human breast adenocarcinoma MCF-7 cells by prodelphinidin B-2,3,3′-di-O-gallate from *Myrica rubra* via Fas-mediated pathway. J Pharm Pharmacol 2004;56:1399–406.
[35] Huang Q, Shen HM, Ong CN. Inhibitory effect of emodin on tumor invasion through suppression of activator protein-1 and nuclear factor-kappaB. Biochem Pharmacol 2004;68:361–71.
[36] Micheau O, Lens S, Gaide O, Alevizopoulos K, Tschopp J. NF-kappaB signals induce the expression of c-FLIP. Mol Cell Biol 2001;21:5299–305.
[37] Thome M, Tschopp J. Regulation of lymphocyte proliferation and death by FLIP. Nat Rev Immunol 2001;1:50–8.
[38] Chang L, Kamata H, Solinas G, Luo JL, Maeda S, et al. The E3 ubiquitin ligase itch couples JNK activation to TNFalpha-induced cell death by inducing c-FLIP(L) turnover. Cell 2006;124:601–13.
[39] Luo X, Budihardjo I, Zou H, Slaughter C, Wang X. Bid a Bcl2 interacting protein, mediates cytochrome c release from mitochondria in response to activation of cell surface death receptors. Cell 1998;94:481–90.

[40] Li H, Zhu H, Xu CJ, Yuan J. Cleavage of BID by caspase 8 mediates the mitochondrial damage in the Fas pathway of apoptosis. Cell 1998;94:491–501.
[41] Desagher S, Martinou JC. Mitochondria as the central control point of apoptosis. Trends Cell Biol 2000;10:369–77.
[42] Hanahan D, Weinberg RA. The hallmarks of cancer. Cell 2000;100:57–70.
[43] Liu FT, Goff LK, Hao JH, Newland AC, Jia L. Increase in the ratio of mitochondrial Bax/Bcl-XL induces Bax activation in human leukemic K562 cell line. Apoptosis 2004;9:377–84.